

Causal Effect Estimation under Networked Interference without Networked Unconfoundedness Assumption

Weilin Chen, Ruichu Cai^{*}, *Senior Member, IEEE*, Jie Qiao, Yuguang Yan, José Miguel Hernández-Lobato

Abstract—Estimating causal effects under networked interference from observational data is a crucial yet challenging problem. Most existing methods mainly rely on the networked unconfoundedness assumption, which guarantees the identification of networked effects. However, this assumption is often violated due to the latent confounders inherent in observational data, thereby hindering the identification of networked effects. To address this issue, we leverage the rich interaction patterns between units in networks, which provide valuable information for recovering these latent confounders. Building on this insight, we develop a confounder recovery framework that explicitly characterizes three categories of latent confounders in networked settings: those affecting only the unit, those affecting only the unit’s neighbors, and those influencing both. Based on this framework, we design a networked effect estimator using identifiable representation learning techniques. From a theoretical standpoint, we prove the identifiability of all three types of latent confounders and, by leveraging the recovered confounders, establish a formal identification result for networked effects. Extensive experiments validate our theoretical findings and demonstrate the effectiveness of the proposed method.

Index Terms—Causal effects, networked interference, latent confounders, identifiability.

I. INTRODUCTION

ESTIMATING causal effects in the presence of networked interference is a crucial yet challenging problem across various domains, including human ecology [1], advertising [2], and epidemiology [3]. The fundamental difficulty lies in that interference between units inherently violates the Stable Unit Treatment Value Assumption (SUTVA), which underpins classical causal inference. For example, when evaluating the effect of a flu vaccine on individual infection rates, a standard causal inference approach assumes that an individual’s infection risk depends only on their own vaccination status. In reality, vaccination induces herd immunity: vaccinating one person may reduce the infection risks of others, leading to indirect

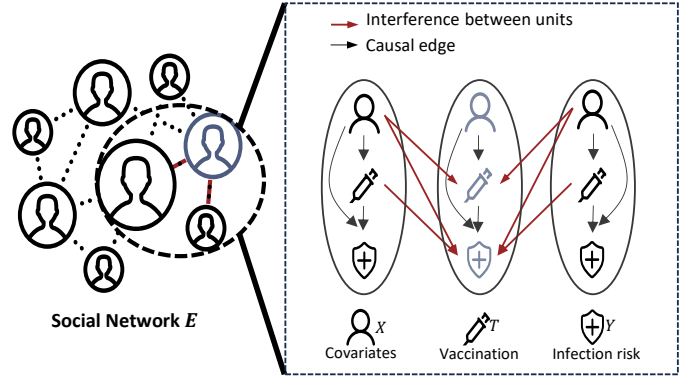


Fig. 1. A toy example showing networked interference between units. The networked interference introduces the interaction between units, i.e., the solid red arrows. Such arrows violate the traditional SUTVA assumption, leading to the non-identifiable problem.

or spillover effects (Figure 1). Such a violation of SUTVA introduces bias into traditional causal inference methods, rendering standard estimands inapplicable [4]. To model the interference between units, prior studies focus on estimating three kinds of networked effects: *main effects* (effects of units’ own treatments), *spillover effects* (effects of units’ treatments on other units), and *total effects* (combined main and spillover effects).

To estimate causal effects from observational networked data, a series of methods have been developed under the networked unconfoundedness assumption. This assumption posits that no latent confounders exist beyond the observed covariates and the covariates of neighboring units. Under this assumption, [4] proposes the joint generalized propensity score for effect estimation and establishes the identification of network effects. Subsequent works introduce balanced representation techniques to construct conditional outcome estimators for effect estimation [5]–[7] and develop doubly robust estimators to improve the robustness of network effect estimation [8], [9] under networked interference.

However, the networked unconfoundedness assumption is often violated in real-world scenarios, significantly limiting the effectiveness of existing methods. For example, in the case of flu vaccination, whether a person chooses to get vaccinated may depend on their income level or their family’s financial situation. However, such socioeconomic factors are often difficult to measure directly due to privacy concerns or

Weilin Chen is with the School of Computer Science, Guangdong University of Technology, Guangzhou, 510006, China (e-mail: chenweilin.chn@gmail.com).

Ruichu Cai is with the School of Computer Science, Guangdong University of Technology, Guangzhou, 510006, China and Peng Cheng Laboratory, Shenzhen, China (e-mail: cairuichu@gmail.com).

Jie Qiao and Yuguang Yan are with the School of Computer Science, Guangdong University of Technology, Guangzhou, 510006, China (e-mail: qiaojie.chn@gmail.com and ygyan@gdut.edu.cn).

José Miguel Hernández-Lobato is with the Department of Engineering, University of Cambridge, Cambridge CB2 1PZ, United Kingdom (e-mail: jmh233@cam.ac.uk).

Corresponding author: Ruichu Cai.

Manuscript received XXX; revised XXX.

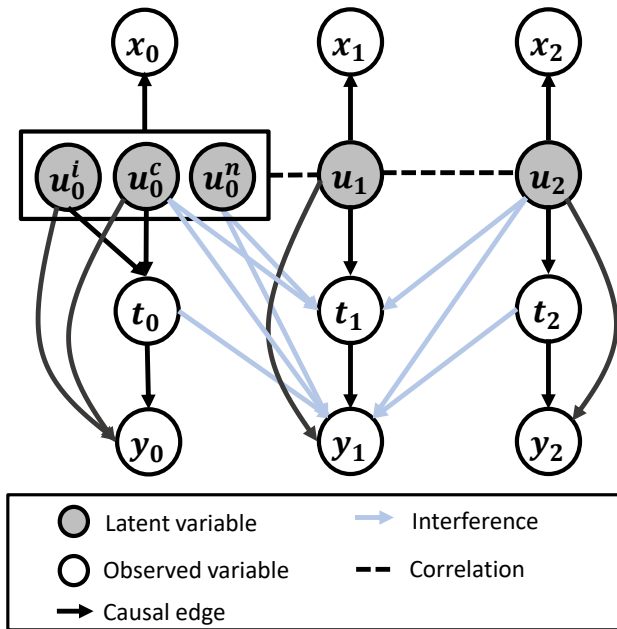


Fig. 2. Assumed causal graph in this paper. x denotes observed proxies, u denotes latent confounders, t denotes the treatment, and y denote the outcome of interest. We assume that latent confounders u contain three types of variables, i.e., u^i affecting the unit itself, u^n affecting the unit’s neighbors, and u^c affecting both.

data collection limitations. Such latent confounders, violating the networked unconfoundedness assumption, bias both main and spillover effect estimation, as well as total effect estimation, fundamentally limiting existing approaches.

To address this limitation, we propose a framework that eliminates the need for the networked unconfoundedness assumption. Specifically, we begin by exploring three categories of latent confounders, illustrated in Figure 2, that hinder the effect identification: u^i affecting only the unit, u^n affecting only neighbors, and u^c influencing both. Rather than assuming networked unconfoundedness, we investigate the identifiability of latent confounders in the presence of networked interference. A key insight of our work is that networked interference itself provides auxiliary information that can be exploited to recover latent confounders. Building on this recovery, we theoretically establish the networked effect identification result and further devise a practical effect estimator under networked interference. Overall, our contribution can be summarized as follows:

- We address the problem of networked effect identification and estimation in the presence of latent confounders, and categorize three types of latent confounders that hinder identification.
- We establish the identifiability of latent confounders by leveraging the auxiliary information revealed by networked interference, and prove that networked effects can be identified.
- We devise a networked effect estimator built upon these theoretical findings. Extensive experiments validate our theoretical results and demonstrate the effectiveness of

the proposed method.

II. RELATED WORKS

Classic Causal Inference has been studied in two languages: the graphical models [10] and the potential outcome framework [11]. The most related method is the propensity score method in the potential outcome framework, e.g., IPW method [12], [13], which is widely applied to many scenarios [14]–[16]. There are also many outcome regression models, including meta-learners [17], neural networks-based works [18]–[21]. By incorporating them, one can construct a doubly robust estimator [22], i.e., the effect estimator is consistent as either the propensity model or the outcome regression model is consistent.

Causal Inference without SUTVA has drawn increasing attention recently. [23] extends the traditional propensity score to account for neighbors’ treatments and features and proposes a generalized Inverse Probability Weighting (IPW) estimator. [4] defines the joint propensity score and then proposes a subclassification-based method. Drawing upon previous works, [24] considers two IPW estimators and derives a closed-form estimator for the asymptotic variance. Based on the representation learning, [6] adds neighborhood exposure and neighbors’ features as additional input variables and applies HSIC to learn balanced representations. [25] uses adversarial learning to learn balanced representations for better effect estimation. [26] proposes a framework to learn causal effects on a hypergraph. [7] proposes a reweighted representation learning method to learn balanced representations. Under networked interference, [9], [27], [28] propose an estimator to achieve DR property. Additionally, [29] proposes SPNet to estimate networked effects without the networked unconfoundedness assumption. However, Most works do assume the unconfoundedness assumption, which might not hold in real-world scenarios. Different from them, we explore the problem of networked effect estimation without the unconfoundedness assumption. While [30] also does not assume this assumption, its estimand only focuses on the effects of the unit’s treatment and and it does not consider the identifiability guarantee of latent confounders. Different from [29], we focus on three kinds of networked effects and establish the latent confounder identifiability results, enabling the effect identification.

Causal Inference without Unconfoundedness Assumption is an important problem since the unconfoundedness assumption is usually violated in observational studies. Classic methods to solve this problem usually assume there exist additional variables, e.g., instrumental variable [31]–[33], proximal variable [34], [35]. Another effective way to address this problem is to recover the latent confounder using representation learning methods. CEVAE [36] assumes that latent confounders can be recovered by their proxies and applies VAE to learn confounders. As a follow-up work, TEDVAE [37] decouples the learned latent confounders into several factors to achieve a more accurate estimation of treatment effects. In the mediation analysis, DMAVAE [38] proposes to recover latent confounders using the VAE similar to CEVAE. Our work is closely related to these works. Different from them, we focus on the causal effect without the unconfoundedness assumption in the presence of

networked interference. We also provide theoretical guarantees for the latent confounder identifiability, which ensures the effectiveness of our estimator.

III. NOTATIONS, ASSUMPTIONS, ESTIMANDS

In this section, we start with the notations used in this work. Let $U \in \mathcal{U}$ be the latent confounders and also let $X \in \mathcal{X}$ be the proxies of latent confounders. Let $T \in \{0, 1\}$ denote a binary treatment, where $T = 1$ indicates a unit receives the treatment (treated) and $T = 0$ indicates a unit receives no treatment (control). Let $Y \in \mathcal{Y}$ be the outcome. We assume that U can be decomposed to U^i affecting the unit itself, U^c affecting the neighbors, and U^n affecting both. Let lowercase letters (e.g., x, y, t) denote the value of random variables. Let lowercase letters with subscript i denote the value of the specified i -th unit. Thus, a network dataset is denoted as $D = (\{x_i, t_i, y_i\}_{i=1}^n, E)$, where E denotes the adjacency matrix of network and n is the total number of units. We denote the set of first-order neighbors of i as \mathcal{N}_i and denote the treatment and feature vectors received by unit i 's neighbors as $t_{\mathcal{N}_i}$ and $x_{\mathcal{N}_i}$. Due to the presence of networked interference, a unit's potential outcome is influenced not only by its treatment but also by its neighbors' treatments, and thus the potential outcome is denoted by $y_i(t_i, t_{\mathcal{N}_i})$. The observed outcome y_i is known as the factual outcome, and the remaining potential outcomes are known as counterfactual outcomes.

Further, following [4], [9], we assume that the dependence between the potential outcome and the neighbors' treatments is through a specified summary function $g: \{0, 1\}^{|\mathcal{N}_i|} \rightarrow [0, 1]$, and let z_i be the neighborhood exposure given by the summary function, i.e., $z_i = g(t_{\mathcal{N}_i})$. We aggregate the information of the neighbors' treatments to obtain the neighborhood exposure by $z_i = \frac{\sum_{j \in \mathcal{N}_i} t_j}{|\mathcal{N}_i|}$. Therefore, the potential outcome $y_i(t_i, t_{\mathcal{N}_i})$ can be denoted as $y_i(t_i, z_i)$, which means that under networked interference, each unit is affected by two kinds of treatments: the binary individual treatment t_i and the continuous neighborhood exposure z_i .

In this paper, our **goal** is to estimate the average dose-response function, as well as the conditional average dose-response function:

$$\begin{aligned} \psi(t, z) &:= \mathbb{E}[Y(t, z)], \\ \mu(t, z, x, x_{\mathcal{N}}) &:= \mathbb{E}[Y(t, z) | X = x, X_{\mathcal{N}} = x_{\mathcal{N}}]. \end{aligned} \quad (1)$$

Based on the above (conditional) average dose-response function, existing works mostly focus on the following causal effects:

Definition 1 (Average Main Effects (AME)). *AME measures the difference in mean outcomes between units assigned to $T = t, Z = 0$ and assigned $T = t', Z = 0$: $\tau^{(t,0),(t',0)} = \psi(t, 0) - \psi(t', 0)$.*

Definition 2 (Average Spillover Effects (ASE)). *ASE measures the difference in mean outcomes between units assigned to $T = 0, Z = z$ and assigned $T = 0, Z = z'$: $\tau^{(0,z),(0,z')} = \psi(0, z) - \psi(0, z')$.*

Definition 3 (Average Total Effects (ATE)). *ATE measures the difference in mean outcomes between units assigned to*

$T = t, Z = z$ and assigned $T = t', Z = z'$: $\tau^{(t,z),(t',z')} = \psi(t, z) - \psi(t', z')$.

Definition 4 (Individual Main Effects (IME)). *IME measures the difference in mean outcomes of a particular unit x_i assigned to $T = t, Z = 0$ and assigned $T = t', Z = 0$: $\tau_i(x_i, x_{\mathcal{N}_i})^{(t,0),(t',0)} = \mu(x_i, x_{\mathcal{N}_i}, t, 0) - \mu(x_i, x_{\mathcal{N}_i}, t', 0)$.*

Definition 5 (Individual Spillover Effects (ISE)). *ISE measures the difference in mean outcomes of a particular unit x_i assigned to $T = 0, Z = z$ and assigned $T = 0, Z = z'$: $\tau_i(x_i, x_{\mathcal{N}_i})^{(0,z),(0,z')} = \mu(x_i, x_{\mathcal{N}_i}, 0, z) - \mu(x_i, x_{\mathcal{N}_i}, 0, z')$.*

Definition 6 (Individual Total Effects (ITE)). *ITE measures the difference in mean outcomes of a particular unit x_i assigned to $T = t, Z = z$ and assigned $T = t', Z = z'$: $\tau_i(x_i, x_{\mathcal{N}_i})^{(t,z),(t',z')} = \mu(x_i, x_{\mathcal{N}_i}, t, z) - \mu(x_i, x_{\mathcal{N}_i}, t', z')$.*

The main effects reflect the effects of changing neighborhood exposure t to t' . The spillover effects reflect the effects of changing neighborhood exposure z to z' . And the total effects represent the combined effect of both main effects and spillover effects.

Throughout this paper, we also assume the following assumptions hold:

Assumption 1 (Networked Consistency). *The potential outcome is the same as the observed outcome under the same individual treatment and neighborhood exposure, i.e., $y_i = y_i(t_i, z_i)$ if unit i actually receives t_i and z_i .*

Assumption 2 (Networked Overlap). *Given any individual and neighbors' features, any treatment pair (t, z) has a non-zero probability of being observed in the data, i.e., $\forall x_i, x_{\mathcal{N}_i}, t_i, z_i, 0 < p(t_i, z_i | x_i, x_{\mathcal{N}_i}) < 1$.*

Assumption 3 (Neighborhood Interference). *The potential outcome of a unit is only affected by their own and the first-order neighbors' treatments, and the effect of the neighbors' treatments is through a summary function: g , i.e., $\forall t_{\mathcal{N}_i}, t'_{\mathcal{N}_i}$ which satisfy $g(t_{\mathcal{N}_i}) = g(t'_{\mathcal{N}_i})$, the following equation holds: $y_i(t_i, t_{\mathcal{N}_i}) = y_i(t_i, t'_{\mathcal{N}_i})$.*

These assumptions are commonly assumed in existing causal inference methods such as [4], [7], [26]. Specifically, Assumption 1 states that there can not be multiple versions of a treatment. Assumption 2 requires that the treatment assignment is nondeterministic. Assumption 3 rules out the dependence of the outcome of unit i , y_i , from the treatment received by units outside its neighbors, i.e., $t_j, j \notin \mathcal{N}_i$, but allows y_i to depend on the treatment received by its neighbors, i.e., $t_k, k \in \mathcal{N}_i$. Also, Assumption 3 states the interaction dependence is assumed to be through a summary function g . Note that Assumption 3 is reasonable in reality for some reason. First, in many applications, units are affected by their first-order neighbors, and the affection of higher-order neighbors is also transported through the first-order neighbors. Second, it is also reasonable that a unit is affected by a specific function of other units' treatment, e.g., how much job-seeking pressure a unit has will depend on how many of its friends receive job training.

Existing methods additionally make the following assumption to ensure effect identification:

Assumption 4 (Networked Unconfoundedness). *The individual treatment and neighborhood exposure are independent of the potential outcome given the unit and neighbors' features, i.e., $\forall t, z$, we have $y_i(t, z) \perp\!\!\!\perp t_i, z_i | x_i, x_{\mathcal{N}_i}$.*

Assumption 4 is an extension of the traditional unconfoundedness assumption and indicates that there is no latent confounder that is the common cause between y_i and t_i, z_i .

Under the assumptions above, the networked effects can be identified [4], [7]. However, Assumption 4 might be too strong to hold, since we can not promise that all confounders are observed in real-world scenarios. Instead, we make a much weaker assumption by incorporating the latent variables as follows:

Assumption 5 (Latent Networked Unconfoundedness). *The individual treatment and neighborhood exposure are independent of the potential outcome given the latent unit's and neighbors' confounders, i.e., $\forall t, z$, we have $y_i(t, z) \perp\!\!\!\perp t_i, z_i | u_i^i, u_i^c, u_{\mathcal{N}_i}^c, u_{\mathcal{N}_i}^n$.*

This assumption allows for the latent confounders u^i, u^c, u^n . Here, we recognize three categories of latent confounders: u_i^i affecting the unit itself, u_i^n affecting the unit's neighbors, and u_i^c affecting both. Thus, what serves as a confounder set under the networked setting is the units' u^i, u^c and the neighbors' $u_{\mathcal{N}_i}^c, u_{\mathcal{N}_i}^n$. This also motivates us to identify each latent confounder for a better estimation. In the next section, we will introduce the identifiability of each latent confounder and further achieve networked effect identification.

IV. LATENT CONFOUNDER IDENTIFIABILITY ENABLES NETWORKED EFFECT IDENTIFICATION

In this section, our goal is to establish networked effect identification in the presence of latent confounders u^i, u^c, u^n . According to Assumption 5, such identification requires access to the latent confounders. This motivates us to employ identifiable causal representation learning techniques for their recovery. To this end, we first introduce the latent confounder identifiability (Theorem 1) and further show that the recovered latent confounders can be disentangled (Theorem 2). Building upon these results, we ultimately establish the identification of networked effects (Theorem 3).

To begin with, following existing identifiable representation learning methods [39], [40], we first introduce the generative model as follows:

$$\begin{aligned} p_{\theta}(X, U | X_{\mathcal{N}}) &= p_{\mathbf{f}}(X | U) p_{\mathbf{T}, \lambda}(U | X_{\mathcal{N}}), \\ p_{\mathbf{f}}(X | U) &= p_{\epsilon}(X - \mathbf{f}(U)), \end{aligned} \quad (2)$$

where $p_{\epsilon}(X - \mathbf{f}(U)) = p(\epsilon)$ is the distribution of additive noise $X = \mathbf{f}(U) + \epsilon$. Further, we assume $p_{\mathbf{T}, \lambda}(U | X_{\mathcal{N}})$ follows the exponential family distribution as follows.

Assumption 6. *The correlation between U and $X_{\mathcal{N}}$ is characterized by:*

$$p_{\mathbf{T}, \lambda}(U | X_{\mathcal{N}}) = \frac{\mathcal{Q}(U)}{\mathcal{C}(X_{\mathcal{N}})} \exp[\mathbf{T}(U)^T \lambda(X_{\mathcal{N}})] \quad (3)$$

where \mathcal{Q} is the base measure, \mathcal{C} is the normalizing constant. The $\lambda(X_{\mathcal{N}})$ is an arbitrary function, and the sufficient statistics $\mathbf{T}(U) = [\mathbf{T}_{\mathbf{f}}(U)^T, \mathbf{T}_{MLP}(U)^T]^T$ contains a) the sufficient statistics $\mathbf{T}_{\mathbf{f}}(U)^T = [\mathbf{T}_1(U_{(1)})^T, \dots, \mathbf{T}_1(U_{(d_U)})^T]^T$ of a factorized exponential family, where all the $\mathbf{T}_i(U_{(i)})$ have dimension larger or equal to 2 and d_U is the dimension of U , and b) the output $\mathbf{T}_{MLP}(U)$ of a neural network with ReLU activations.

This assumption is introduced by [40]. The distribution in Assumption 6 is more flexible than the standard assumed distribution condition in identifiable representation learning (Eq. (7) in [39]). This assumption allows for the case that the different elements of latent confounders are not independent given the conditional set. The term $\mathbf{T}_{MLP}(U)$ does capture arbitrary dependencies between latent variables since the neural network with ReLU activation has universal approximation power.

Now, we formally state the theoretical result of the identifiability of latent confounders.

Theorem 1. *Suppose Assumption 6 holds, and suppose the following conditions hold: (1) The set $\{X \in \mathcal{O} | \varphi_{\epsilon}(X) = 0\}$ has measure zero where φ_{ϵ} is the characteristic function of density p_{ϵ} . (2) \mathbf{f} is injective and has all second-order cross derivatives. (3) The sufficient statistics in $\mathbf{T}_{\mathbf{f}}$ are all twice differentiable and each $\mathbf{T}_{\mathbf{f}}$ has at least one invertible dimension. (4) There exist $k + 1$ distinct values $x_{N_0}, \dots, x_{N_{k+1}}$ such that the matrix*

$$L = (\lambda(x_{N_1}) - \lambda(x_{N_0}), \dots, \lambda(x_{N_{k+1}}) - \lambda(x_{N_0}))$$

of size $k \times k$ is invertible where k is the dimension of \mathbf{T} . Then we learn the true latent variable $U = [U^i, U^c, U^n]^T$ up to a permutation and element-wise transformations.

Proof is given in Appendix A.

Discussion on assumptions: Assumption 6 indicates our theory holds for a rich family of conditional densities [41]. The assumption on the exponential family distribution is not strong, since many well-known distributions belong to this family, including the Gaussian, Uniform, Poisson distributions, and so on. Conditions (1)-(4) are mild and common assumptions in causal representation learning, e.g., [39], [40], [42]. In particular, Condition (3) is motivated by [42] to ensure that the identifiability holds for the recovered latent variables beyond their sufficient statistics. Among these, the most critical is Condition (4), which requires that the auxiliary information be sufficiently informative. In our networked setting, this translates to the existence of enough variability in neighbors' covariates, a condition that is typically satisfied when a sufficiently rich set of covariates is collected, especially if some covariates are continuous.

Theorem 1 shows that, under mild assumptions, the latent confounders can be recovered up to an invertible transformation by utilizing the auxiliary information revealed by networked interference. Specifically, the recovered latent variables $\hat{U}^i, \hat{U}^c, \hat{U}^n$ satisfy $\hat{U}^i, \hat{U}^c, \hat{U}^n = h(U^i, U^c, U^n)$ for some bijective element-wise transformations h . However, the exact correspondence between the recovered dimensions and the

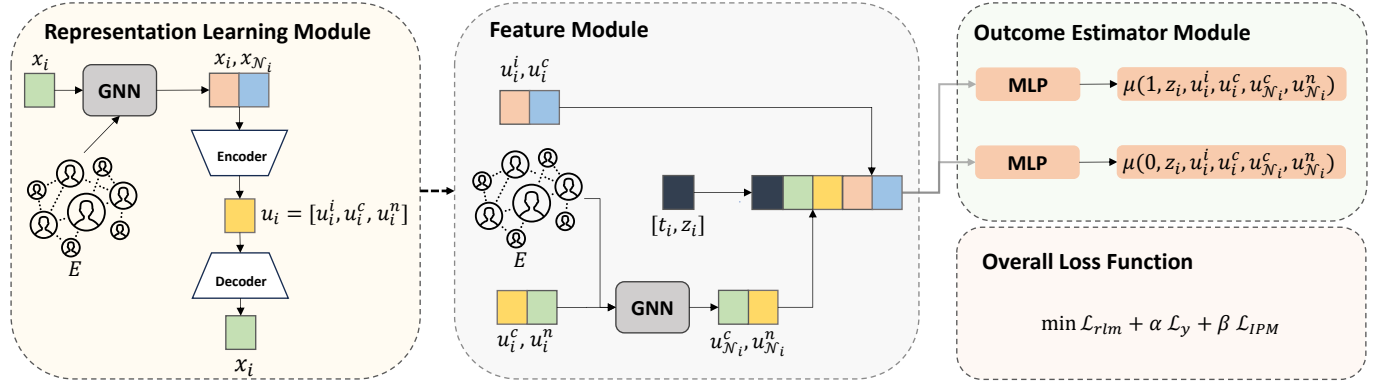


Fig. 3. Model architecture of our proposed method named CaLaNet. The representation learning module aims to learn the latent confounders. The feature module aggregates the information of the confounders of unit i and its neighbor. The outcome estimator module aims to estimate potential outcomes of unit i .

original latent variables U^i, U^c and U^n remains unidentified due to an unknown permutation. This ambiguity, nevertheless, can be resolved by exploiting the asymmetric roles that these latent variables play in the causal structure: U^i only affects the unit itself, U^c only affects the neighbors, and U^n affects both, as shown in the following theorem.

Theorem 2. *Suppose Theorem 1 holds. Then, by maximizing the log-likelihood of Y , i.e., $\max \log p(Y | U^i, U^c, U_{N_i}^c, U_{N_i}^n)$, the latent variables U^i, U^c , and U^n are identifiable up to a permutation and element-wise transformations within each group, respectively.*

Proof is given in Appendix B.

Theorem 2 indicates that the three categories of recovered latent confounders can be further disentangled, i.e., the recovered $\hat{U}^i, \hat{U}^c, \hat{U}^n$ satisfying $\hat{U}^i = h_i(U^i), \hat{U}^c = h_c(U^c), \hat{U}^n = h_n(U^n)$ for some simple functions h_i, h_c, h_n . Based on Theorem 2 above, we can further identify networked effect as follows:

Theorem 3. *Suppose Assumptions 1, 2, 3, 5, and Theorems 1 and 2 hold, the networked effects $\mu(t, z, x, x_{N_i})$ can be identified by:*

$$\begin{aligned} \mu(t, z, x, x_{N_i}) \\ = \mathbb{E}[\mathbb{E}[Y | \hat{U}^i = \hat{u}^i, \hat{U}^c = \hat{u}^c, \hat{U}_{N_i}^c = \hat{u}_{N_i}^c, \hat{U}_{N_i}^n = \hat{u}_{N_i}^n, \\ T = t, Z = z]] \end{aligned} \quad (4)$$

where \hat{u} denotes the recovered latent variables, and similarly for the average effects $\psi(t, z)$.

Proof is given in Appendix C.

Theorem 3 indicates that if we can identify latent confounders, the networked effect is thereby identifiable. This necessitates the utilization of identifiable representation learning techniques for causal inference in the presence of networked interference and latent confounders. Built upon the theoretical findings, in the next section, we propose our practical networked effect estimator that utilizes identifiable causal representation learning techniques.

V. METHODOLOGY

In this section, we devise our networked effect estimator in the presence of latent confounders. Specifically, our estimator contains three modules, including the representation learning module, the feature module, and the outcome estimator module. The representation learning module is built on Theorem 1, aiming to correctly recover three types of latent confounders u^i, u^c, u^n . The feature module is built on Theorems 2 and 3, aggregating the information from units' and neighbors' information. This aggregated information is then input into the outcome estimator module to predict the networked causal effects. Overall, our model architecture is shown in Figure 3.

A. Representation Learning Module

Following existing work [6], [9], [25], [43], we use Graph Convolution Networks (GCN [44], [45]) to aggregate the information of covariates of unit i and its neighbors, i.e., x_i, x_{N_i} :

$$h_{i,1}^{neigh} = \sigma\left(\sum_{j \in N_i} \frac{1}{\sqrt{d_i d_j}} W_1^T x_j\right), \quad (5)$$

$$h_{i,2} = MLP_1(h_{i,1}^{neigh}, x_i),$$

where $\sigma(\cdot)$ is a nonlinear activation function, d_i is the degrees of unit i , W_1 is the learning weight matrix of GCN, and MLP_1 is a multilayer perceptron (MLP). Here, the representation $h_{i,2}$ serves as x_i and x_{N_i} .

Then, given x_i and x_{N_i} , we employ the identifiable representation learning technique to recover latent confounders. Specifically, according to Assumption 6, we parametrize the prior following [40], [42]:

$$\begin{aligned} p(u_i | x_{N_i}) \\ = \langle MLP_2(u_i), MLP_3(h_{i,2}) \rangle + \langle [u_i, u_i^2], MLP_4(h_{i,2}) \rangle \end{aligned} \quad (6)$$

where $u_i = [u_i^i, u_i^c, u_i^n]$ and $MLP_2(u_i)$ serves as T_{MLP} , the concatenated $[u_i, u_i^2]$ serves as T_f , $MLP_3(h_{i,2})$ serves as λ_{MLP} , and $MLP_4(h_{i,2})$ serves as λ_f in Assumption 6.

As for the encoder, the variational approximation of the posterior is defined as:

$$q(u_i^i, u_i^c, u_i^n | x_i, x_{\mathcal{N}_i}) = \prod_{i=0}^{d_U} \mathcal{N}(\mu = \hat{\mu}_{u_i}, \sigma^2 = \hat{\sigma}_{u_i}^2), \quad (7)$$

where $\hat{\mu}_{u_i}$ and $\hat{\sigma}_{u_i}^2$ are the mean and variance of the Gaussian distribution parametrized by MLPs using $h_{i,2}$ as input, and d_U is the dimension of U .

As for the decoder, for a continuous outcome, we parametrize the probability distribution as a Gaussian distribution with its mean given by an MLP and a fixed variance v^2 . For a discrete outcome, we use a Bernoulli distribution parametrized by an MLP similarly:

$$p(x_i | u_i^i, u_i^c, u_i^n) = \prod_{i=0}^{d_X} \mathcal{N}(\mu = \hat{\mu}_x, \sigma^2 = v_x^2) \quad (8)$$

or $p(x_i | u_i^i, u_i^c, u_i^n) = \prod_{i=0}^{d_X} \mathbf{Bern}(\pi = \hat{\pi}_x),$

where for the continuous case $\hat{\mu}_x$ is the mean of the Gaussian distribution parametrized by an MLP using the sampled u_i^i, u_i^c, u_i^n from posterior as input and v_x^2 is the fixed variance of Gaussian distribution, and for the discrete case $\hat{\pi}_x$ is the mean of Bernoulli distribution similarly parametrized by an MLP, and here d_X is the dimension of X .

In this module, we use the negative variational Evidence Lower BOund (ELBO) as the loss function, defined as

$$\mathbf{ELBO} = \mathbb{E}_{q(u^i, u^c, u^n | x.x_{\mathcal{N}})} [\log p(x | u^i, u^c, u^n) + \log p(u^i, u^c, u^n | x_{\mathcal{N}}) - \log q(u^i, u^c, u^n | x.x_{\mathcal{N}})]. \quad (9)$$

Detailed ELBO devotions are given in Appendix D.

Since the prior belongs to a multivariate exponential family distribution with unknown normalization constant \mathcal{C} , it is infeasible to learn T and λ by optimizing the KL-divergence term in Eq. (9). Therefore, we utilize the widely used score matching technique [46] for training unnormalized densities to learn the parameters of T and λ by minimizing

$$\mathcal{L}_{sm} = \mathbb{E}_{q(u^i, u^c, u^n | x.x_{\mathcal{N}})} [\|\nabla_u \log q(u^i, u^c, u^n | x.x_{\mathcal{N}}) - \nabla_u \log p(u^i, u^c, u^n | x_{\mathcal{N}})\|^2], \quad (10)$$

where ∇ is the gradient operator. Therefore, the loss function for the representation learning module is

$$\mathcal{L}_{rlm} = \mathbb{E}_{q(u^i, u^c, u^n | x.x_{\mathcal{N}})} [-\log p(x | u^i, u^c, u^n) + \|\nabla_u \log q(u^i, u^c, u^n | x.x_{\mathcal{N}}) - \nabla_u \log p(u^i, u^c, u^n | x_{\mathcal{N}})\|^2], \quad (11)$$

B. Feature Module and Outcome Estimator Module

After obtaining u^i, u^c, u^n , we can aggregate the necessary information for the effect estimation. Specifically, in the feature module, we first aggregate the neighbors' u^c, u^n to obtain $u_{\mathcal{N}}^c, u_{\mathcal{N}}^n$ via GCN:

$$h_{i,3}^{neigh} = \sigma \left(\sum_{j \in \mathcal{N}_i} \frac{1}{\sqrt{d_i d_j}} W_2^T [u_j^c, u_j^n] \right),$$

$$h_{i,4} = MLP_1(h_{i,3}^{neigh}, u_i^i, u_i^c),$$

where $\sigma(\cdot)$ is a nonlinear activation function, d_i is the degrees of unit i , W_2 is the learning weight matrix of GCN. Here, $h_{i,3}^{neigh}$ serves as the neighbor latent confounders $[u_{\mathcal{N}_i}^c, u_{\mathcal{N}_i}^n]$ and $h_{i,4}$ serves as the whole confounders $[u_i^i, u_i^c, u_{\mathcal{N}_i}^c, u_{\mathcal{N}_i}^n]$, used to prediction the outcomes y_i .

Then, we use $h_{i,4}$ and t_i, z_i together to estimate y_i of treated and control groups respectively, i.e.,

$$\mu^{NN}(t_i, z_i, u_i^i, u_i^c, u_{\mathcal{N}_i}^c, u_{\mathcal{N}_i}^n) = \begin{cases} MLP_3(z_i, h_{i,4}), & t_i = 1 \\ MLP_4(z_i, h_{i,4}), & t_i = 0 \end{cases},$$

and the loss function is

$$\mathcal{L}_y = -\sum_{i=1}^n (y_i - \mu^{NN}(t_i, z_i, x_i, x_{\mathcal{N}_i}))^2. \quad (12)$$

Moreover, inspired by [7], [25], we further consider a balancing regularization term to learn a balanced representation as our loss:

$$\mathcal{L}_{IPM} = \text{IPM}(p(h_{i,4}, t_i, z_i), p(h_{i,4})p(t_i, z_i)), \quad (13)$$

where $\text{IPM}(p, q) = \sup_{g \in \mathcal{G}} | \int_{\mathcal{X}} g(x)(p(x) - q(x))dx |$ is the integral probability metric, measuring the distance between two distribution p, q , which can be implemented by Wasserstein Distance. Here the samples from $p(h_{i,4})p(t_i, z_i)$ is obtained by randomly permuting the observed treatment pairs t_i and z_i .

Overall, our final loss function is

$$\mathcal{L}_{all} = \mathcal{L}_{rlm} + \alpha \mathcal{L}_{IPM} + \beta \mathcal{L}_y, \quad (14)$$

where α and β are the hyperparameters that control the weights of the respective loss terms.

We denote our method as **CaLaNet** (Causal representation learning-based Latent-confounder recovery for Networked effect estimation).

VI. EXPERIMENTS

In this section, we verify the effectiveness of our method, CaLaNet, and further evaluate the correctness of the theories using the commonly used semisynthetic datasets. In particular, we aim to answer the following research questions (RQs):

- **RQ1:** How does the proposed method perform compared with existing methods?
- **RQ2:** Can the proposed model correctly recover the latent confounders?
- **RQ3:** Does our model stably perform well under different choices of hyperparameters?

A. Experimental Setup

To begin with, we first introduce our experimental setup, including the used datasets, the compared baselines, and the used metrics.

1) *Datasets:* We consider two widely used semisynthetic datasets, BlogCatalog and Flickr, to verify the effectiveness of our estimator. We further use a synthetic dataset to validate the correctness of our theories, i.e., whether our method can correctly recover latent confounders.

Following existing works [9], [25], [43], [47], we use two semisynthetic datasets to evaluate our proposed method:

TABLE I
EXPERIMENTAL RESULTS ON BC(HOMO) DATASET. THE TOP RESULT IS HIGHLIGHTED IN BOLD, AND THE RUNNER-UP IS UNDERLINED.

Methods	$\varepsilon_{average}$						$\varepsilon_{individual}$					
	Within Sample			Out-of Sample			Within Sample			Out-of Sample		
	AME	ASE	ATE	AME	ASE	ATE	IME	ISE	ITE	IME	ISE	ITE
TARNET+z	0.1573 \pm 0.0405	0.0824 \pm 0.0149	0.2046 \pm 0.0193	0.1492 \pm 0.0370	0.0855 \pm 0.0147	0.1982 \pm 0.0380	0.2096 \pm 0.0250	0.1161 \pm 0.0159	0.2444 \pm 0.0239	0.2809 \pm 0.0507	0.1209 \pm 0.0152	0.3062 \pm 0.0627
CFR+z	0.0788 \pm 0.0096	0.1157 \pm 0.0076	0.2323 \pm 0.0106	<u>0.0770</u> \pm 0.0099	0.1157 \pm 0.0075	0.2306 \pm 0.0106	<u>0.0796</u> \pm 0.0091	0.1158 \pm 0.0076	0.2325 \pm 0.0106	0.1000 \pm 0.0388	0.1157 \pm 0.0075	0.2405 \pm 0.0166
GEst	0.1872 \pm 0.0672	0.2369 \pm 0.0607	0.1422 \pm 0.0562	0.1955 \pm 0.0611	0.2391 \pm 0.0617	0.1302 \pm 0.0524	0.2307 \pm 0.0493	0.2603 \pm 0.0586	0.1877 \pm 0.0495	0.2388 \pm 0.0431	0.2623 \pm 0.0592	0.1790 \pm 0.0440
ND+z	0.2375 \pm 0.0450	<u>0.0316</u> \pm 0.0104	0.0790 \pm 0.0226	0.2380 \pm 0.0458	<u>0.0323</u> \pm 0.0122	0.0768 \pm 0.0254	0.2377 \pm 0.0448	<u>0.0321</u> \pm 0.0101	0.0792 \pm 0.0226	0.2477 \pm 0.0460	<u>0.0379</u> \pm 0.0099	0.1068 \pm 0.0172
NetEst	0.0989 \pm 0.0735	0.0428 \pm 0.0487	0.0596 \pm 0.0291	0.0995 \pm 0.0725	0.0425 \pm 0.0487	0.0599 \pm 0.0286	0.0992 \pm 0.0732	0.0431 \pm 0.0485	0.0602 \pm 0.0290	0.1130 \pm 0.0617	0.0553 \pm 0.0443	0.0660 \pm 0.0254
RRNet	0.0884 \pm 0.0495	0.0445 \pm 0.0158	0.0768 \pm 0.0239	0.0892 \pm 0.0505	0.0447 \pm 0.0160	0.0782 \pm 0.0253	0.0915 \pm 0.0462	0.0452 \pm 0.0153	0.0865 \pm 0.0260	<u>0.0917</u> \pm 0.0491	0.0453 \pm 0.0159	0.0887 \pm 0.0282
SPNet+z	<u>0.0802</u> \pm 0.0632	0.0446 \pm 0.0155	0.0570 \pm 0.0188	0.0931 \pm 0.0607	0.0394 \pm 0.0215	<u>0.0385</u> \pm 0.0183	0.1153 \pm 0.0482	0.0741 \pm 0.0109	0.1094 \pm 0.0274	0.1358 \pm 0.0566	0.0604 \pm 0.0145	0.0933 \pm 0.0342
TNet	0.1045 \pm 0.0610	0.0502 \pm 0.0559	<u>0.0473</u> \pm 0.0229	0.1045 \pm 0.0610	0.0502 \pm 0.0559	0.0473 \pm 0.0229	0.1045 \pm 0.0610	0.0502 \pm 0.0559	<u>0.0473</u> \pm 0.0229	0.1045 \pm 0.0610	0.0502 \pm 0.0559	<u>0.0473</u> \pm 0.0229
CaLaNet	0.0551 \pm 0.0423	0.0279 \pm 0.0279	0.0288 \pm 0.0150	0.0549 \pm 0.0426	0.0278 \pm 0.0279	0.0288 \pm 0.0150	0.0554 \pm 0.0418	0.0279 \pm 0.0279	0.0289 \pm 0.0149	0.0551 \pm 0.0424	0.0278 \pm 0.0279	0.0288 \pm 0.0149

- **BlogCatalog (BC)** is an online community where users post blogs. In this dataset, each unit is a blogger and each edge is the social link between units. The features are bag-of-words representations of keywords in bloggers' descriptions.
- **Flickr** is an online social network where users can share images and videos. In this dataset, each unit is a user, and each edge is the social relationship between units. The features are the list of tags of units' interests.

We reuse the original covariates as the latent confounders and then divide them into u^i, u^c, u^n . We generate the proxies x_i using $x_i = w_1 u_i + e_i$ where w_1 are randomly sampled from Uniform distribution $\mathcal{U}(0.5, 1)$ and $e_{x,i}$ is standard Gaussian noise. Then given the latent confounder u_i^i, u_i^c, u_i^n of unit i , the treatments are simulated by

$$t_i = \begin{cases} 1 & \text{if } tpt_i > \overline{tpt}, \\ 0 & \text{else,} \end{cases}$$

where \overline{tpt} is the average of all tpt_i , and $tpt_i = pt_i + pt_{N_i}$, and $pt_i = \text{Sigmoid}(w_2 \times [u_i^i, u_i^c])$, and $pt_{N_i} = \frac{1}{|N_i|} \sum_j^{j \in N_i} \text{Sigmoid}(w_3 \times [u_i^c, u_i^n])$ serves as the neighbors influences. Here, w_2 and w_3 are randomly generated weight vectors that mimic the causal mechanism from the latent confounders to treatments. Then, z_i can be directly obtained by network topology E and t_{N_i} .

We then modify the data generation of outcome y in [25] using the latent confounders u_i instead of observed x_i :

$$y_i(t_i, z_i) = t_i + z_i + po_i + 0.5 \times po_{N_i} + e_{y,i},$$

where $e_{y,i}$ is a Gaussian noise term, and $po_i = \text{Sigmoid}(w_4 \times u_i + w_5 \times u_c)$, and po_{N_i} is the averages of $\text{Sigmoid}(w_6 \times u_c + w_7 \times u_n)$. Here, w_4, w_5, w_6 , and w_7 are all randomly generated weight vectors that mimic the causal mechanism from the confounders to outcomes. We denote this dataset as **BC(homo)** and **Flickr(homo)**¹ since this generation of y only measures the homogeneous causal effects.

¹Original datasets are available at <https://github.com/songjiang0909/Causal-Inference-on-Networked-Data>.

Also following [9], we consider the data generation of outcome y with heterogeneous effects:

$$y_i(t_i, z_i) = t_i + z_i + po_i + 0.5 \times po_{N_i} + t_i(po_i + 0.5 \times po_{N_i}) + t_i(0.5 \times po_i + po_{N_i}) + e_{y,i},$$

and the datasets are denoted as **BC(hete)** and **Flickr(hete)**.

Due to the space limit, we leave the detailed data generation process of the synthetic dataset in Appendix E.

2) *Baselines*: We denote our method as **CaLaNet**². We compare CaLaNet with several state-of-the-art baselines as follows:

- **TARNET+z**: Original Tarnet [48] uses two-heads neural networks, serving as T-Learner-like estimator, to estimate causal effects under no interference assumption. We modify TARNET by additionally inputting the exposure z_i .
- **CFR+z**: Original CFR [48] uses two-heads neural networks with an MMD term to achieve counterfactual regression under no interference assumption. We modify CFR by additionally inputting the exposure z_i .
- **ND+z**: Original ND [43] propose network deconfounder framework by using network information under no interference assumption. We modify ND by additionally inputting the exposure z_i .
- **GEst** [6]: GESt, based on CFR, uses GCN to aggregate the features of neighbors and input the exposure z_i to estimate causal effects under networked interference.
- **NetEst** [25]: NetEst learns balanced representation via adversarial learning for networked causal effect estimation.
- **RRNet** [7]: RRNet combines the representation learning and reweighting techniques in its network to estimate causal effects under interference.
- **SPNet+z** [29]: SPNet estimates the effect of the individual treatment t_i while keeping the neighbor exposure z_i unchanged. We adapt SPNet to our setting by incorporating z_i as an additional input.

²Our code will be available upon acceptance.

TABLE II
EXPERIMENTAL RESULTS ON BC(HETE) DATASET. THE TOP RESULT IS HIGHLIGHTED IN BOLD, AND THE RUNNER-UP IS UNDERLINED.

Methods	$\varepsilon_{average}$						$\varepsilon_{individual}$					
	Within Sample			Out-of Sample			Within Sample			Out-of Sample		
	AME	ASE	ATE	AME	ASE	ATE	IME	ISE	ITE	IME	ISE	ITE
TARNET+z	0.2538 \pm 0.1127	0.1657 \pm 0.0563	0.3866 \pm 0.0711	0.2619 \pm 0.1054	0.1701 \pm 0.0594	0.4044 \pm 0.1334	0.3455 \pm 0.0654	0.2122 \pm 0.0558	0.4605 \pm 0.0720	0.5590 \pm 0.2643	0.2207 \pm 0.0510	0.6349 \pm 0.3280
CFR+z	0.1580 \pm 0.0189	0.2071 \pm 0.0237	0.4067 \pm 0.0407	0.1559 \pm 0.0203	0.2076 \pm 0.0245	0.4061 \pm 0.0449	0.1825 \pm 0.0129	0.2092 \pm 0.0233	0.4316 \pm 0.0351	0.2058 \pm 0.0432	0.2098 \pm 0.0242	0.4422 \pm 0.0456
GEst	0.2734 \pm 0.1240	0.4257 \pm 0.0973	0.2916 \pm 0.1119	0.2722 \pm 0.1308	0.4277 \pm 0.1012	0.2873 \pm 0.1220	0.3334 \pm 0.1082	0.4592 \pm 0.0934	0.3546 \pm 0.0947	0.3832 \pm 0.1474	0.4612 \pm 0.0972	0.3958 \pm 0.1486
ND+z	0.4124 \pm 0.0702	<u>0.0451</u> \pm 0.0201	0.1330 \pm 0.0205	0.4111 \pm 0.0737	0.0486 \pm 0.0206	0.1326 \pm 0.0261	0.4226 \pm 0.0673	<u>0.0562</u> \pm 0.0146	0.1941 \pm 0.0246	0.4330 \pm 0.0662	0.0666 \pm 0.0137	0.2211 \pm 0.0321
NetEst	0.2301 \pm 0.0784	0.0799 \pm 0.0453	0.1296 \pm 0.0594	0.2252 \pm 0.0729	0.0785 \pm 0.0441	0.1221 \pm 0.0594	0.2479 \pm 0.0737	0.0859 \pm 0.0433	0.1960 \pm 0.0444	0.2485 \pm 0.0761	0.0923 \pm 0.0433	0.1988 \pm 0.0435
RRNet	0.1628 \pm 0.1183	0.0476 \pm 0.0416	0.0919 \pm 0.0581	0.1636 \pm 0.1162	<u>0.0474</u> \pm 0.0424	0.0961 \pm 0.0640	0.1967 \pm 0.0979	0.0591 \pm 0.0364	0.1719 \pm 0.0485	0.1974 \pm 0.0960	<u>0.0595</u> \pm 0.0365	0.1764 \pm 0.0505
SPNet+z	<u>0.0706</u> \pm 0.0738	0.0714 \pm 0.0256	0.1169 \pm 0.0317	<u>0.0805</u> \pm 0.0716	0.0671 \pm 0.0230	0.0841 \pm 0.0419	0.1743 \pm 0.0338	0.1054 \pm 0.0138	0.2209 \pm 0.0288	<u>0.1901</u> \pm 0.0480	0.0906 \pm 0.0190	0.2012 \pm 0.0480
TNet	0.1216 \pm 0.0864	0.0537 \pm 0.0524	<u>0.0429</u> \pm 0.0301	0.1257 \pm 0.0727	0.0537 \pm 0.0511	0.0481 \pm 0.0269	<u>0.1731</u> \pm 0.0450	0.0655 \pm 0.0465	0.1458 \pm 0.0175	0.1915 \pm 0.0542	0.0650 \pm 0.0458	<u>0.1740</u> \pm 0.0621
CaLaNet	0.0701 \pm 0.0571	0.0321 \pm 0.0239	0.0401 \pm 0.0264	0.0691 \pm 0.0550	0.0305 \pm 0.0243	0.0396 \pm 0.0265	0.1224 \pm 0.0310	0.0458 \pm 0.0181	<u>0.1481</u> \pm 0.0210	0.1216 \pm 0.0300	0.0452 \pm 0.0178	0.1493 \pm 0.0185

TABLE III
EXPERIMENTAL RESULTS ON FLICKR(HOMO) DATASET. THE TOP RESULT IS HIGHLIGHTED IN BOLD, AND THE RUNNER-UP IS UNDERLINED.

Methods	$\varepsilon_{average}$						$\varepsilon_{individual}$					
	Within Sample			Out-of Sample			Within Sample			Out-of Sample		
	AME	ASE	ATE	AME	ASE	ATE	IME	ISE	ITE	IME	ISE	ITE
TARNET+z	0.0783 \pm 0.0418	0.0874 \pm 0.0213	0.2025 \pm 0.0396	0.0976 \pm 0.0506	0.0724 \pm 0.0184	0.1356 \pm 0.0587	0.1362 \pm 0.0254	0.1103 \pm 0.0194	0.2358 \pm 0.0383	1.0869 \pm 1.2258	0.1011 \pm 0.0185	1.0889 \pm 1.2270
CFR+z	0.0579 \pm 0.0247	0.0785 \pm 0.0070	0.1651 \pm 0.0121	0.0507 \pm 0.0192	0.0783 \pm 0.0070	0.1581 \pm 0.0097	0.0599 \pm 0.0240	0.0786 \pm 0.0070	0.1654 \pm 0.0120	0.3465 \pm 0.4615	0.0786 \pm 0.0069	0.4102 \pm 0.4278
GEst	0.1551 \pm 0.0130	0.2475 \pm 0.0476	0.0805 \pm 0.0325	0.1511 \pm 0.0137	0.2494 \pm 0.0470	0.0805 \pm 0.0278	0.1779 \pm 0.0122	0.2656 \pm 0.0378	0.1268 \pm 0.0160	0.2867 \pm 0.2172	0.2677 \pm 0.0372	0.2471 \pm 0.2352
ND+z	0.1416 \pm 0.0240	<u>0.0204</u> \pm 0.0093	0.0478 \pm 0.0216	0.1435 \pm 0.0364	<u>0.0226</u> \pm 0.0101	0.0485 \pm 0.0236	0.1427 \pm 0.0246	<u>0.0221</u> \pm 0.0090	0.0501 \pm 0.0178	0.3849 \pm 0.2395	0.0348 \pm 0.0078	0.3453 \pm 0.2772
NetEst	0.0515 \pm 0.0538	0.0355 \pm 0.0317	0.0715 \pm 0.0381	0.0470 \pm 0.0500	0.0338 \pm 0.0330	0.0529 \pm 0.0395	0.0844 \pm 0.0406	0.0566 \pm 0.0253	0.1043 \pm 0.0312	0.2934 \pm 0.3001	0.2809 \pm 0.3387	0.3068 \pm 0.1860
RRNet	<u>0.0296</u> \pm 0.0123	0.0251 \pm 0.0172	<u>0.0199</u> \pm 0.0179	<u>0.0296</u> \pm 0.0123	0.0251 \pm 0.0172	<u>0.0199</u> \pm 0.0179	<u>0.0296</u> \pm 0.0123	0.0251 \pm 0.0172	<u>0.0199</u> \pm 0.0179	<u>0.0296</u> \pm 0.0123	<u>0.0251</u> \pm 0.0172	<u>0.0199</u> \pm 0.0179
SPNet+z	0.0366 \pm 0.0359	0.0604 \pm 0.0371	0.1267 \pm 0.0655	0.0451 \pm 0.0332	0.0445 \pm 0.0300	0.0865 \pm 0.0410	0.0639 \pm 0.0273	0.0980 \pm 0.0269	0.1877 \pm 0.0546	0.0834 \pm 0.0342	0.0694 \pm 0.0234	0.1309 \pm 0.0500
TNet	0.0319 \pm 0.0249	0.0274 \pm 0.0309	0.0735 \pm 0.0240	0.0299 \pm 0.0231	0.0277 \pm 0.0313	0.0715 \pm 0.0214	0.0347 \pm 0.0282	0.0276 \pm 0.0313	0.0752 \pm 0.0263	0.0561 \pm 0.0648	0.0286 \pm 0.0331	0.0918 \pm 0.0555
CaLaNet	0.0223 \pm 0.0159	0.0147 \pm 0.0068	0.0151 \pm 0.0127	0.0222 \pm 0.0158	0.0148 \pm 0.0069	0.0154 \pm 0.0128	0.0223 \pm 0.0159	0.0149 \pm 0.0069	0.0152 \pm 0.0127	0.0223 \pm 0.0158	0.0148 \pm 0.0068	0.0155 \pm 0.0129

- **TNet** [9]: TNet utilizes targeted learning techniques into its neural networks model to estimate causal effects under networked interference in a double robust manner.

3) *Metrics*: In this paper, we use the Mean Absolute Error (MAE) on AME, ASE, and ATE as our metric, i.e., $\varepsilon_{average} = |\hat{\tau} - \tau|$, where τ and $\hat{\tau}$ are the average causal effect and estimated one. We also use the Rooted Precision in Estimation of Heterogeneous Effect on IME, ASE, and ITE, $\varepsilon_{individual} = \sqrt{\frac{1}{n} \sum_{i=1}^n (\hat{\tau}_i - \tau_i)^2}$, where τ_i and $\hat{\tau}_i$ are the individual causal effect and estimated one. The mean and standard deviation of these metrics via 5 times running are reported. Note that our main estimands are AME, ASE, and ATE in this paper.

B. Experimental Analyses

1) *RQ1: Effectiveness of CaLaNet*: As shown in Tables I, II, III, and IV, we have conducted experiments by running our proposed method, CaLaNet, and several baselines. Overall, our CaLaNet outperforms all methods consistently with smaller estimation errors in all metrics, indicating the effectiveness of our methods. Specifically, compared with the baselines, our methods perform better in terms of both average and heterogeneous treatment effect estimation, with smaller errors

and standard deviation. This means our CaLaNet is not only accurate for networked effect estimation but also performs stably. This is reasonable since most existing methods do not consider the latent confounders that hinder the effect identification, while our method utilizes representation learning techniques and thereby achieves superior performances with recovered latent confounders. In particular, SPNet+z also considers latent confounders. However, it has no theoretical guarantee for the latent confounder recovery, and thus underperforms our CaLaNet. Hence, the results in III, Table I, II, and IV showcase the effectiveness of our proposed CaLaNet.

2) *RQ2: Correctness of Representation Learning*: To validate the correctness of our representation learning method, we conduct experiments in the simulated dataset and visualize the recovered latent confounders $\hat{U}^i, \hat{U}^c, \hat{U}^n$ alongside ground-truth ones U^i, U^c, U^n in Figure 4. We also report the corresponding Matthews Correlation Coefficient (MCC) results in Table V. As shown in Figure 4, the diagonal scatter plots (top-left, middle, and bottom-right) show strong alignments, indicating that each recovered latent confounder ($\hat{U}^i, \hat{U}^c, \hat{U}^n$) closely corresponds to its ground-truth counterpart (U^i, U^c, U^n). In contrast, the off-diagonal scatter plots exhibit no obvious correlation, suggesting that the latent factors are

TABLE IV
EXPERIMENTAL RESULTS ON FLICKR(HETE) DATASET. THE TOP RESULT IS HIGHLIGHTED IN BOLD, AND THE RUNNER-UP IS UNDERLINED.

Methods	$\varepsilon_{average}$						$\varepsilon_{individual}$					
	Within Sample			Out-of Sample			Within Sample			Out-of Sample		
	AME	ASE	ATE	AME	ASE	ATE	IME	ISE	ITE	IME	ISE	ITE
TARNET+z	0.1315 \pm 0.0740	0.1673 \pm 0.0423	0.3590 \pm 0.0785	0.1554 \pm 0.1110	0.1319 \pm 0.0307	0.2728 \pm 0.1321	0.2320 \pm 0.0432	0.2042 \pm 0.0479	0.4254 \pm 0.0802	1.5274 \pm 1.6256	0.1760 \pm 0.0351	1.5957 \pm 1.5779
CFR+z	0.1131 \pm 0.0476	0.1437 \pm 0.0081	0.2960 \pm 0.0182	0.0998 \pm 0.0458	0.1412 \pm 0.0085	0.2789 \pm 0.0309	0.1445 \pm 0.0407	0.1463 \pm 0.0083	0.3242 \pm 0.0224	0.5946 \pm 0.7379	0.1448 \pm 0.0087	0.7104 \pm 0.6761
GEst	0.3283 \pm 0.0426	0.4717 \pm 0.1336	0.1074 \pm 0.0255	0.3356 \pm 0.0270	0.4723 \pm 0.1312	0.0969 \pm 0.0099	0.3697 \pm 0.0386	0.5123 \pm 0.1231	0.2178 \pm 0.0214	0.7124 \pm 0.6463	0.5144 \pm 0.1202	0.5914 \pm 0.7073
ND+z	0.2420 \pm 0.0330	0.0293 \pm 0.0113	0.0852 \pm 0.0365	0.2433 \pm 0.0539	0.0318 \pm 0.0134	0.0785 \pm 0.0422	0.2571 \pm 0.0348	0.0430 \pm 0.0040	0.1607 \pm 0.0188	0.5156 \pm 0.2180	0.0669 \pm 0.0059	0.4720 \pm 0.2580
NetEst	0.0530 \pm 0.0423	0.0452 \pm 0.0351	0.0723 \pm 0.0319	0.0466 \pm 0.0322	0.0565 \pm 0.0454	0.0818 \pm 0.0379	0.1145 \pm 0.0278	0.0667 \pm 0.0267	0.1660 \pm 0.0163	0.6855 \pm 0.2607	0.5353 \pm 0.2507	0.5625 \pm 0.1367
RRNET	0.0441 \pm 0.0196	0.0280 \pm 0.0153	<u>0.0367</u> \pm 0.0243	0.0446 \pm 0.0183	0.0292 \pm 0.0165	0.0329 \pm 0.0255	0.0940 \pm 0.0166	0.0401 \pm 0.0105	0.1373 \pm 0.0188	0.0952 \pm 0.0153	0.0436 \pm 0.0100	0.1419 \pm 0.0202
SPNet+z	0.0429 \pm 0.0461	0.0885 \pm 0.0509	0.2359 \pm 0.0724	0.0509 \pm 0.0404	0.0555 \pm 0.0264	0.1483 \pm 0.0573	0.1296 \pm 0.0241	0.1593 \pm 0.0314	0.3538 \pm 0.0513	0.1827 \pm 0.1051	0.1053 \pm 0.0208	0.2879 \pm 0.0823
TNet	<u>0.0411</u> \pm 0.0238	<u>0.0206</u> \pm 0.0073	<u>0.0282</u> \pm 0.0297	<u>0.0417</u> \pm 0.0237	<u>0.0196</u> \pm 0.0098	<u>0.0268</u> \pm 0.0314	<u>0.0936</u> \pm 0.0170	<u>0.0338</u> \pm 0.0065	<u>0.1360</u> \pm 0.0210	<u>0.0950</u> \pm 0.0157	<u>0.0361</u> \pm 0.0074	<u>0.1415</u> \pm 0.0223
CaLaNet	0.0283 \pm 0.0223	0.0135 \pm 0.0070	0.0257 \pm 0.0099	0.0316 \pm 0.0206	0.0146 \pm 0.0074	0.0217 \pm 0.0091	0.0892 \pm 0.0111	0.0302 \pm 0.0053	0.1334 \pm 0.0144	0.0911 \pm 0.0099	0.0334 \pm 0.0055	0.1383 \pm 0.0151

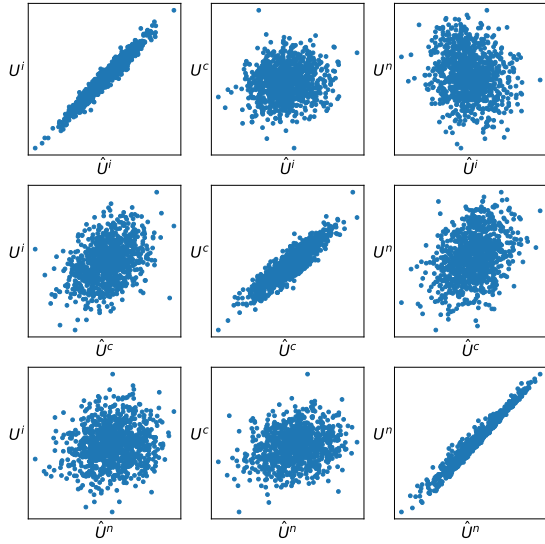


Fig. 4. The figure presents scatter plots visualizing the relationship between the recovered latent confounders and ground-truth latent confounders U^i , U^c , and U^n .

TABLE V
MCC RESULTS BETWEEN THE RECOVERED LATENT CONFOUNDERS AND GROUND-TRUTH LATENT CONFOUNDERS U^i , U^c , AND U^n .

	\hat{U}^i	\hat{U}^c	\hat{U}^n
U^i	0.9729	0.1742	0.2032
U^c	0.3796	0.9090	0.3616
U^n	0.1879	0.2420	0.9901

well disentangled. Similar findings are reflected in the MCC results in Table V, where the corresponding recovered and ground-truth confounders show high correlation, while the non-corresponding ones do not. These results confirm that the proposed representation learning method effectively recovers

the latent confounders, in line with the theoretical identifiability guarantees.

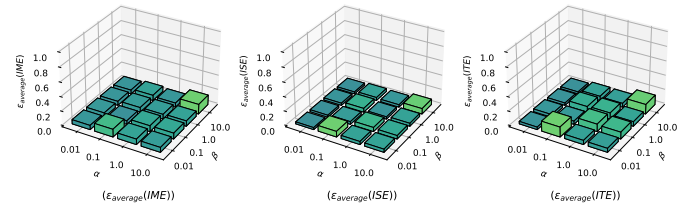


Fig. 5. Hyperparameter sensitivity result regarding individual effect estimation error on BC(homo) dataset.

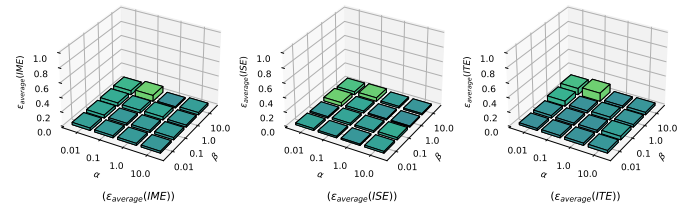


Fig. 6. Hyperparameter sensitivity result regarding individual effect estimation error on Flickr(homo) dataset.

3) *RQ3: Stability Regarding Hyperparameters:* We evaluate the stability of CaLaNet under varying hyperparameter settings for α and β , choosing values from the set $\{0.01, 0.1, 1.0, 10.0\}$. The results on individual effect estimation errors for both datasets are presented in Figures 5 and 6, with comprehensive results available in Appendix E. As illustrated in the figures, CaLaNet demonstrates relatively stable performance overall, suggesting that it is not highly sensitive to the choice of α and β within a moderate range. Also, we observe that excessively small or large values (e.g., $\alpha = 0.01$ or $\beta = 10.0$) can degrade performance, which is expected due to the resulting imbalance across different loss components. In summary, CaLaNet performs well under reasonably balanced loss weights and shows reasonable stability across a wide range of hyperparameters.

VII. CONCLUSION

In this paper, we tackle the challenge of identifying and estimating causal effects under networked interference in the presence of latent confounders. Specifically, we systematically categorize three distinct types of latent confounders that hinder networked effect identification. To address this issue, we propose leveraging the networked information to achieve the identifiability of latent confounders. Based on this recovery, we theoretically establish conditions under which networked causal effects become identifiable. Building on these theoretical insights, we develop an effective estimator grounded in identifiable representation learning. Extensive experiments empirically validate both the theoretical results and the practical effectiveness of our proposed method.

ACKNOWLEDGMENTS

This research was supported in part by National Science and Technology Major Project (2021ZD0111501), National Science Fund for Excellent Young Scholars (62122022), Natural Science Foundation of China (U24A20233, 62206064, 62206061, 62476163, 62406078), Guangdong Basic and Applied Basic Research Foundation (2023B1515120020), and CCF-DiDi GAIA Collaborative Research Funds (CCF-DiDi GAIA 202311).

VIII. REFERENCES SECTION

REFERENCES

- [1] P. J. Ferraro, J. N. Sanchirico, and M. D. Smith, "Causal inference in coupled human and natural systems," *Proceedings of the National Academy of Sciences*, vol. 116, no. 12, pp. 5311–5318, 2019.
- [2] P. Parshakov, I. Naidenova, and A. Barajas, "Spillover effect in promotion: Evidence from video game publishers and esports tournaments," *Journal of Business Research*, vol. 118, pp. 262–270, 2020.
- [3] B. G. Barkley, M. G. Hudgens, J. D. Clemens, M. Ali, and M. E. Emch, "Causal inference from observational studies with clustered interference, with application to a cholera vaccine study," *Annals of Applied Statistics*, vol. 14, no. 3, pp. 1432–1448, 2020.
- [4] L. Forastiere, E. M. Airoldi, and F. Mealli, "Identification and estimation of treatment and interference effects in observational studies on networks," *Journal of the American Statistical Association*, vol. 116, no. 534, pp. 901–918, 2021.
- [5] A. Chin, "Regression adjustments for estimating the global treatment effect in experiments with interference," *Journal of Causal Inference*, vol. 7, no. 2, p. 20180026, 2019.
- [6] Y. Ma and V. Tresp, "Causal inference under networked interference and intervention policy enhancement," in *International Conference on Artificial Intelligence and Statistics*. PMLR, 2021, pp. 3700–3708.
- [7] R. Cai, Z. Yang, W. Chen, Y. Yan, and Z. Hao, "Generalization bound for estimating causal effects from observational network data," in *Proceedings of the 32nd ACM International Conference on Information and Knowledge Management*, ser. CIKM '23. New York, NY, USA: Association for Computing Machinery, 2023, p. 163–172. [Online]. Available: <https://doi.org/10.1145/3583780.3614892>
- [8] L. Liu, M. G. Hudgens, B. Saul, J. D. Clemens, M. Ali, and M. E. Emch, "Doubly robust estimation in observational studies with partial interference," *Stat*, vol. 8, no. 1, p. e214, 2019.
- [9] W. Chen, R. Cai, Z. Yang, J. Qiao, Y. Yan, Z. Li, and Z. Hao, "Doubly robust causal effect estimation under networked interference via targeted learning," *arXiv preprint arXiv:2405.03342*, 2024.
- [10] J. Pearl, *Causality*. Cambridge university press, 2009.
- [11] D. B. Rubin, "Estimating causal effects of treatments in randomized and nonrandomized studies." *Journal of educational Psychology*, vol. 66, no. 5, p. 688, 1974.
- [12] P. R. Rosenbaum and D. B. Rubin, "The central role of the propensity score in observational studies for causal effects," *Biometrika*, vol. 70, no. 1, pp. 41–55, 1983.
- [13] P. R. Rosenbaum, "Model-based direct adjustment," *Journal of the American Statistical Association*, vol. 82, no. 398, pp. 387–394, 1987.
- [14] P. R. Rosenbaum and D. B. Rubin, "Constructing a control group using multivariate matched sampling methods that incorporate the propensity score," *The American Statistician*, vol. 39, no. 1, pp. 33–38, 1985.
- [15] F. Li, K. L. Morgan, and A. M. Zaslavsky, "Balancing covariates via propensity score weighting," *Journal of the American Statistical Association*, vol. 113, no. 521, pp. 390–400, 2018.
- [16] R. Cai, W. Chen, Z. Yang, S. Wan, C. Zheng, X. Yang, and J. Guo, "Long-term causal effects estimation via latent surrogates representation learning," *Neural Networks*, vol. 176, p. 106336, 2024. [Online]. Available: <https://www.sciencedirect.com/science/article/pii/S089368024002600>
- [17] S. R. Künzel, J. S. Sekhon, P. J. Bickel, and B. Yu, "Metalearners for estimating heterogeneous treatment effects using machine learning," *Proceedings of the national academy of sciences*, vol. 116, no. 10, pp. 4156–4165, 2019.
- [18] F. Johansson, U. Shalit, and D. Sontag, "Learning representations for counterfactual inference," in *International conference on machine learning*. PMLR, 2016, pp. 3020–3029.
- [19] S. Assaad, S. Zeng, C. Tao, S. Datta, N. Mehta, R. Henao, F. Li, and L. Carin, "Counterfactual representation learning with balancing weights," in *International Conference on Artificial Intelligence and Statistics*. PMLR, 2021, pp. 1972–1980.
- [20] K. Kuang, P. Cui, H. Zou, B. Li, J. Tao, F. Wu, and S. Yang, "Data-driven variable decomposition for treatment effect estimation," *IEEE Transactions on Knowledge and Data Engineering*, vol. 34, no. 5, pp. 2120–2134, 2022.
- [21] A. Wu, J. Yuan, K. Kuang, B. Li, R. Wu, Q. Zhu, Y. Zhuang, and F. Wu, "Learning decomposed representations for treatment effect estimation," *IEEE Transactions on Knowledge and Data Engineering*, vol. 35, no. 5, pp. 4989–5001, 2023.
- [22] J. M. Robins, A. Rotnitzky, and L. P. Zhao, "Estimation of regression coefficients when some regressors are not always observed," *Journal of the American statistical Association*, vol. 89, no. 427, pp. 846–866, 1994.
- [23] L. Liu, M. G. Hudgens, and S. Becker-Dreps, "On inverse probability-weighted estimators in the presence of interference," *Biometrika*, vol. 103, no. 4, pp. 829–842, 2016.
- [24] T. Lee, A. L. Buchanan, N. V. Katenka, L. Forastiere, M. E. Halloran, S. R. Friedman, and G. Nikolopoulos, "Estimating causal effects of hiv prevention interventions with interference in network-based studies among people who inject drugs," *arXiv preprint arXiv:2108.04865*, 2021.
- [25] S. Jiang and Y. Sun, "Estimating causal effects on networked observational data via representation learning," in *Proceedings of the 31st ACM International Conference on Information & Knowledge Management*, 2022, pp. 852–861.
- [26] J. Ma, M. Wan, L. Yang, J. Li, B. Hecht, and J. Teevan, "Learning causal effects on hypergraphs," in *Proceedings of the 28th ACM SIGKDD Conference on Knowledge Discovery and Data Mining*, 2022, pp. 1202–1212.
- [27] V. McNealis, E. E. Moodie, and N. Dean, "Doubly robust estimation of causal effects in network-based observational studies," *arXiv preprint arXiv:2302.00230*, 2023.
- [28] J. Liu, F. Ye, and Y. Yang, "Nonparametric doubly robust estimation of causal effect on networks in observational studies," *Stat*, vol. 12, no. 1, p. e549, 2023.
- [29] Q. Huang, J. Ma, J. Li, R. Guo, H. Sun, and Y. Chang, "Modeling interference for individual treatment effect estimation from networked observational data," *ACM Trans. Knowl. Discov. Data*, vol. 18, no. 3, Dec. 2023. [Online]. Available: <https://doi.org/10.1145/3628449>
- [30] Z. Zhao, Y. Bai, R. Xiong, Q. Cao, C. Ma, N. Jiang, F. Wu, and K. Kuang, "Learning individual treatment effects under heterogeneous interference in networks," *ACM Transactions on Knowledge Discovery from Data*, vol. 18, no. 8, pp. 1–21, 2024.
- [31] J. Pearl *et al.*, "Models, reasoning and inference," *Cambridge, UK: CambridgeUniversityPress*, vol. 19, no. 2, p. 3, 2000.
- [32] J. H. Stock and F. Trebbi, "Retrospectives: Who invented instrumental variable regression?" *Journal of Economic Perspectives*, vol. 17, no. 3, pp. 177–194, 2003.
- [33] A. Wu, K. Kuang, B. Li, and F. Wu, "Instrumental variable regression with confounder balancing," in *International Conference on Machine Learning*. PMLR, 2022, pp. 24 056–24 075.
- [34] W. Miao, Z. Geng, and E. J. Tchetgen Tchetgen, "Identifying causal effects with proxy variables of an unmeasured confounder," *Biometrika*, vol. 105, no. 4, pp. 987–993, 2018.

- [35] E. J. Tchetgen Tchetgen, A. Ying, Y. Cui, X. Shi, and W. Miao, “An introduction to proximal causal inference,” *Statistical Science*, vol. 39, no. 3, pp. 375–390, 2024.
- [36] C. Louizos, U. Shalit, J. M. Mooij, D. Sontag, R. Zemel, and M. Welling, “Causal effect inference with deep latent-variable models,” *Advances in neural information processing systems*, vol. 30, 2017.
- [37] W. Zhang, L. Liu, and J. Li, “Treatment effect estimation with disentangled latent factors,” in *Proceedings of the AAAI Conference on Artificial Intelligence*, 2021, pp. 10923–10930.
- [38] Z. Xu, D. Cheng, J. Li, J. Liu, L. Liu, and K. Wang, “Disentangled representation for causal mediation analysis,” in *Proceedings of the AAAI Conference on Artificial Intelligence*, vol. 37, 2023, pp. 10666–10674.
- [39] I. Khemakhem, D. Kingma, R. Monti, and A. Hyvarinen, “Variational autoencoders and nonlinear ica: A unifying framework,” in *International conference on artificial intelligence and statistics*. PMLR, 2020, pp. 2207–2217.
- [40] C. Lu, Y. Wu, J. M. Hernández-Lobato, and B. Schölkopf, “Invariant causal representation learning for out-of-distribution generalization,” in *International Conference on Learning Representations*, 2022. [Online]. Available: <https://openreview.net/forum?id=-e4EXDWXnSn>
- [41] M. J. Wainwright and M. I. Jordan, “Graphical models, exponential families, and variational inference,” *Found. Trends Mach. Learn.*, vol. 1, no. 1–2, p. 1–305, Jan. 2008. [Online]. Available: <https://doi.org/10.1561/2200000001>
- [42] Y. Zhu, J. Ma, L. Wu, Q. Guo, L. Hong, and J. Li, “Causal effect estimation with mixed latent confounders and post-treatment variables,” in *The Thirteenth International Conference on Learning Representations*, 2025. [Online]. Available: <https://openreview.net/forum?id=qe1CsfnN1W>
- [43] R. Guo, J. Li, and H. Liu, “Learning individual causal effects from networked observational data,” in *Proceedings of the 13th International Conference on Web Search and Data Mining*, 2020, pp. 232–240.
- [44] M. Defferrard, X. Bresson, and P. Vandergheynst, “Convolutional neural networks on graphs with fast localized spectral filtering,” *Advances in neural information processing systems*, vol. 29, 2016.
- [45] T. N. Kipf and M. Welling, “Semi-supervised classification with graph convolutional networks,” in *International Conference on Learning Representations*, 2016.
- [46] P. Vincent, “A connection between score matching and denoising autoencoders,” *Neural computation*, vol. 23, no. 7, pp. 1661–1674, 2011.
- [47] J. Ma, R. Guo, C. Chen, A. Zhang, and J. Li, “Deconfounding with networked observational data in a dynamic environment,” in *Proceedings of the 14th ACM International Conference on Web Search and Data Mining*, 2021, pp. 166–174.
- [48] F. D. Johansson, U. Shalit, N. Kallus, and D. Sontag, “Generalization bounds and representation learning for estimation of potential outcomes and causal effects,” 2021.

IX. BIOGRAPHY SECTION



Weilin Chen received his B.S. degree in Software Engineering in 2020 and his Ph.D. degree in Computer Science in 2025, both from Guangdong University of Technology, Guangzhou, China. In 2024, he was a visiting student at the University of Cambridge, UK. His current research interests include causal inference and its applications. He has served as a program committee member or reviewer for leading conferences and journals, including ICML, ICLR, NeurIPS, AISTATS, and IEEE TNNLS, among others.



Ruichu Cai (M’17) is currently a professor in the school of computer science and the director of the data mining and information retrieval laboratory, Guangdong University of Technology. He received his B.S. degree in applied mathematics and Ph.D. degree in computer science from South China University of Technology in 2005 and 2010, respectively.

His research interests cover various topics, including causality, deep learning, and their applications. He was a recipient of the National Science Fund for Excellent Young Scholars, the Natural Science Award of Guangdong, and so on awards. He has served as the area chair of ICML 2022, NeurIPS 2022, and UAI 2022, senior PC for AAAI 2019–2022, IJCAI 2019–2022, and so on. He is now a senior member of CCF and IEEE.



Jie Qiao received his Ph.D. from Guangdong University of Technology, School of Computer Science, in 2021. He is currently an Assistant Professor at the School of Computer Science, Guangdong University of Technology.

His research interests cover various topics, including causality and its application. He has served as the program committee of ICML 2022–2025, NeurIPS 2022–2025, ICLR 2024–2025, AAAI 2021–2025, IJCAI 2023–2025, UAI 2022–2025, and so on.



Yuguang Yan received the B.S. and Ph.D. degrees in the School of Software Engineering from South China University of Technology, China, in 2013 and 2019, respectively. He is currently with the School of Computer Science, Guangdong University of Technology, China. He was a Post-doctoral Fellow at The University of Hong Kong from 2019 to 2021. His current research interests include optimal transport, causal inference, and graph data analysis.



José Miguel Hernández-Lobato is Professor of Machine Learning at the Department of Engineering in the University of Cambridge, UK. Before joining Cambridge as faculty, he was a postdoctoral fellow at Harvard University, and before this, also a postdoctoral research associate at the University of Cambridge. Jose Miguel completed his Ph.D. and M.Phil. in Computer Science at Universidad Autónoma de Madrid (Spain), where he also obtained a B.Sc. in Computer Science from this institution, with a special prize to the best academic record on graduation. José Miguel's research interests are on probabilistic machine learning, with a focus on deep generative models, Bayesian optimization, approximate inference, causal inference, Bayesian neural networks and applications of these methods to real-world problems.